Fronto-Parietal Anatomical Connections Influence the Modulation of Conscious Visual Perception by High-Beta Frontal Oscillatory Activity

Romain Quentin[4], Lorena Chanes[1], Marine Vernet[1] and Antoni Valero-Cabré[1,2,3]

[1]Institut du Cerveau et de la Moelle Epinière, ICM, CNRS UMR 7225, INSERM U 1127 and Université Pierre et Marie Curie, Paris, France, [2]Laboratory for Cerebral Dynamics Plasticity and Rehabilitation, Boston University School of Medicine, Boston, MA, USA, [3]Cognitive Neuroscience and Information Technology Research Program, Open University of Catalonia (UOC), Barcelona, Spain and [4]Centre de NeuroImagerie de Recherche - CENIR, Institut du Cerveau et de la Moelle epiniére, Groupe Hospitalier Pitié-Salpêtrière, Paris, France

Address correspondence to Dr Antoni Valero-Cabré, MD, PhD, CNRS, INSERM, Université Pierre et Marie Curie, ICM, Equipe Cognition, Neuro-imagerie et maladies du Cerveau; Groupe de Dynamiques Cérébrales, Plasticité et Rééducation, Hôpital de la Salpêtrière, 47 boulevard de l'Hôpital, 75651 Paris Cedex 13, France. Email: avalerocabre@gmail.com; avalero@bu.edu

May white matter connectivity influence rhythmic brain activity underlying visual cognition? We here employed diffusion imaging to reconstruct the fronto-parietal white matter pathways in a group of healthy participants who displayed frequency-specific ameliorations of visual sensitivity during the entrainment of high-beta oscillatory activity by rhythmic transcranial magnetic stimulation over their right frontal eye field. Our analyses reveal a strong tract-specific association between the volume of the first branch of the superior longitudinal fasciculus and improvements of conscious visual detection driven by frontal beta oscillation patterns. These data indicate that the architecture of specific white matter pathways has the ability to influence the distributed effects of rhythmic spatio-temporal activity, and suggest a potentially relevant role for long-range connectivity in the synchronization of oscillatory patterns across fronto-parietal networks subtending the modulation of conscious visual perception.

Keywords: brain, oscillations, synchronization, conscious visual perception, noninvasive neurostimulation, visuo-spatial attention, white matter anatomy

Introduction

Correlational approaches employed to investigate the influence of white matter fasciculi on human behaviors have revealed tract-specific influences on cognitive processes, such as choice selection, visuo-spatial orienting, and motor training (Tuch et al. 2005; Scholz et al. 2009; Thiebaut de Schotten et al. 2011). Similarly, observations in animals (Valero-Cabré et al. 2005, 2007) and humans (Quentin et al. 2013) have strongly suggested an association between interindividual differences of specific white matter pathways linking the targeted region and key postsynaptic sites with the behavioral impact induced by focal patterns of noninvasive neurostimulation.

Here, we specifically addressed whether the behavioral effects derived from frequency-specific oscillation patterns induced by rhythmic noninvasive brain stimulation may be particularly impacted by the individual characteristics of white matter projections. We employed a transcranial magnetic stimulation (TMS) dataset from a recent experiment in which we tested the impact on conscious visual performance of short frequency-specific 30-Hz bursts delivered to the right frontal eye field (FEF) prior to the onset of a low-contrast visual Gabor, displayed either to the right or left of a fixation cross (Chanes et al. 2013) (Fig. 1a,b). Importantly, we aimed to use frequency-tailored patterns to enhance local oscillations

(Romei et al. 2010; Thut et al. 2011) and entrain synchronization throughout a fronto-parietal dorsal network, considered key for spatial attentional orienting and the top-down modulation of visual perception (Chanes et al. 2012).

Stimulation site and frequency were matched to those of a nonhuman primate study reporting the engagement of high-beta (22–34 Hz) activity across frontal and parietal dorsal regions during a visual search task involving endogenous attentional orienting (Buschman and Miller 2007). In our population, short episodes of 30-Hz spatio-temporal activity delivered to the right FEF prior to target onset induced statistically significant improvements of perceptual sensitivity in a visual detection task, which were absent when control nonfrequency-specific stimulation patterns were employed (Chanes et al. 2013). Interestingly, despite robust statistically significant group effects, across-subject performance differences were observed (Fig. 1c). As we recently demonstrated for single TMS pulses (Quentin et al. 2013), we hypothesized that such behavioral variability could largely emerge (among other potential factors) from interindividual white matter connectivity differences modulating the distributed impact of frequency-specific bursts throughout fronto-parietal cortical networks (Buschman and Miller 2007).

Diffusion images acquired prior to the experiments were used to track with a deterministic method based on spherical deconvolution (Dell'acqua et al. 2010) the 3 branches of the superior longitudinal fasciculus (SLF) in both hemispheres of each participant's brain. The SLF I is the dorsal-most white matter pathway linking the superior parietal lobule encompassing the intraparietal sulcus (IPS), with the middle and superior frontal gyrus (Thiebaut de Schotten et al. 2011), where the FEF is located. The cortical connection sites of this pathway correspond to the dorsal attentional orienting network involved in endogenous spatial orienting (Kincade et al. 2005). This system can engage in high-beta oscillatory activity and fronto-parietal synchrony during top-down attentional control in monkeys (Buschman and Miller 2007) and humans (Phillips and Takeda 2009), and has been causally associated with the modulation of conscious vision (Chanes et al. 2013). The SLF II, located in the central core of the white matter above the insula, links the angular gyrus to both the superior and lateral prefrontal regions (Makris et al. 2005) and has been considered a potential link between the ventral and dorsal attentional orienting networks (Thiebaut de Schotten et al. 2012). Finally, the SLF III associates the supramarginal gyrus and the temporo-parietal junction to both ventral
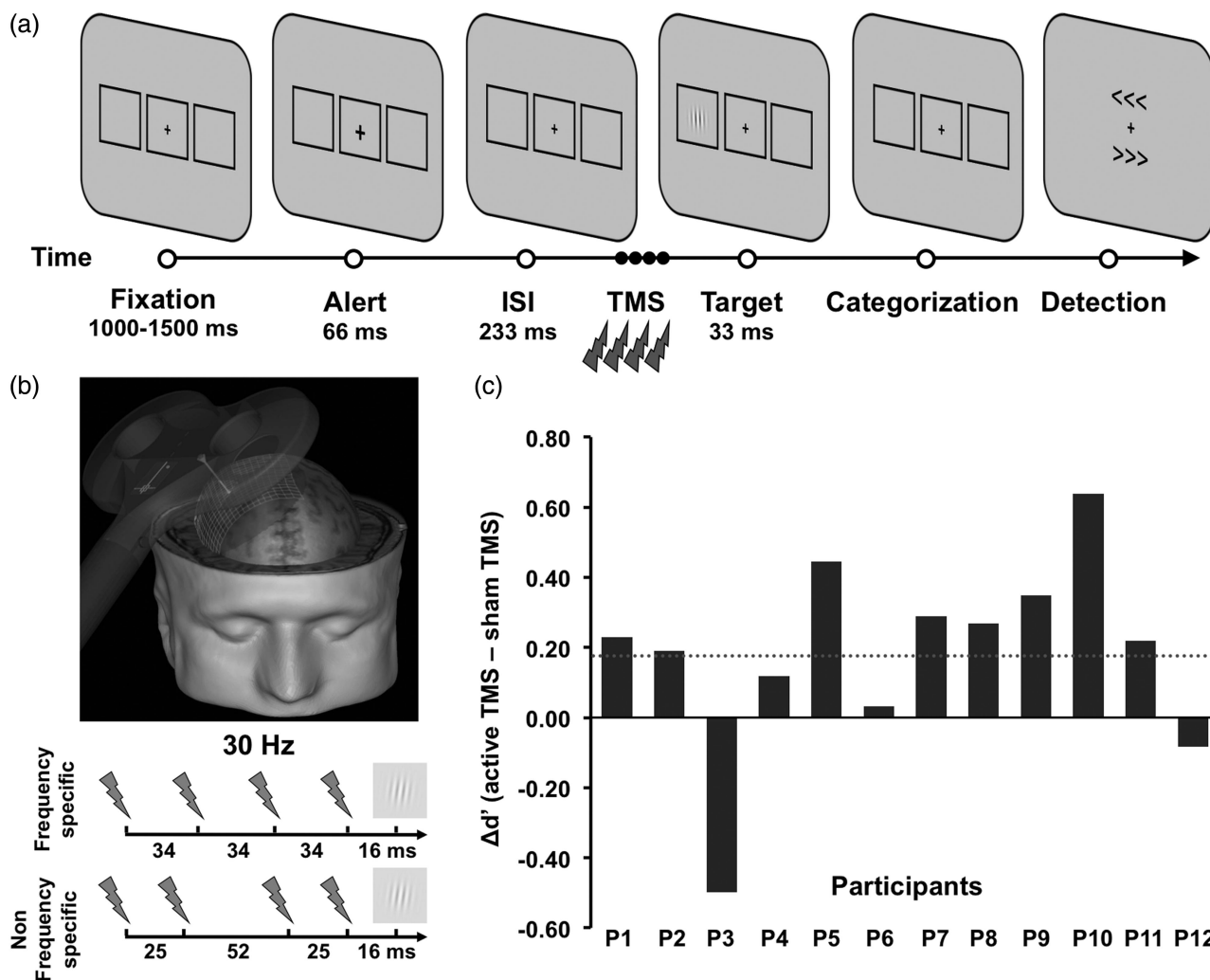
Figure 1. Visual performance task and rhythmic right frontal oscillation patterns used in the study. (*a*) Sequence of events during a representative trial of the visual performance paradigm employed in the study. After variable fixation time, participants were requested to discriminate the orientation of the Gabor lines and indicate if they had or not detected the presence of the target and where (right or left) did this appear in the visual field. (*b*) TMS coil positioning on the right FEF region; temporal distribution of "frequency-specific" and "nonfrequency-specific" spatio-temporal oscillation patterns delivered prior to the Gabor target onset. (*c*) Individual levels of conscious visual detection performance modulated by frequency-specific, high-beta (30 Hz) patterns in each of the 12 participants of our study (from P1 to P12). Data are presented as perceptual sensitivity gains (Δd′, d′ active TMS − d′ sham TMS) induced by FEF beta oscillations in the conscious visual detection task. Positive and negative values indicate visual sensitivity (d′) increases and decreases, respectively. The horizontal discontinuous gray line signals the mean level of statistically significant visual sensitivity effects induced by high-beta frontal oscillations in the whole group of participants. Note that in spite of significant group d′ improvements, participants showed interindividual differences in the magnitude and the direction of such effects.

premotor and prefrontal regions. These areas, which are involved in automatic reorienting toward an unexpected event, correspond to the ventral attentional orienting network (Corbetta et al. 2008; Chica et al. 2011).

Materials and Methods

Study Participants

The data used in this study were extracted from a recently published behavioral-TMS dataset (Chanes et al. 2013). Twelve of 14 participants of the original study for which we had diffusion magnetic resonance imaging (MRI) sequences (7 males and 5 females; mean age = 24.7 ± 3.7 years; minimum age = 20 years; maximum age = 31 years) were included in our analyses. Participants were naïve to both, the purpose of the experiment and the uses of TMS. They freely provided informed written consent prior to their participation and were compensated for taking part in the study. The protocol was reviewed by the INSERM (Institut National de la Santé et la Recherche Scientifique) ethical

committee and approved by an Institutional Review Board (CPP Ile de France 1).

Behavioral Paradigm and TMS

Each trial started with a gray (luminance: 75 cd/m²) resting screen (17″ wide, 1024 × 768) displayed during 2500 ms followed by a central fixation cross (0.5 × 0.5°) lasting randomly between 1000 and 1500 ms, and presented along 3 rectangular placeholders outlined in black (6.0° × 5.5°), 1 located centrally and 2 placed laterally, to the right and left of the fixation cross. Then, the fixation cross became sligthly larger (0.7 × 0.7°) for 66 ms to alert participants of an upcoming event and following an interstimulus interval (ISI) of 233 ms, a low-contrast Gabor stimulus (2 cycles/degree spatial frequency, 3.0° diameter, 0.3° of SD, minimum and maximum Michelson contrast of 0.031 and 0.283, respectively) with lines tilted 1° to 10° to the left or to the right (vertical orientation = 0°) appeared at the center of 1 of the 2 lateral placeholders for 33 ms (Fig. 1*a*). Prior to the session, participants performed a titration block, which started with a high-contrast stimulus. Every 20 trials, target contrast and line tilting were adjusted (in steps of 0.07 Michelson contrast and 1° of tilting, respectively), so that

approximately 50% of the displayed targets were consciously reported ("detection" task) and 65–85% of the latter were correctly discriminated ("discrimination" task). Throughout the experiment, stimulus parameters were also automatically adjusted every 20 trials to maintain this same titration levels.

Prior to target onset, 4 pulse 30-Hz bursts of sham or active TMS ("frequency-specific" patterns, interpulse intervals between first—second, second–third, and third—fourth pulses = 34, 34, and 34 ms, respectively) were delivered on the right FEF. To verify the behavioral impact of pattern frequency on visual performance, the latter were compared in separate blocks with sham and active nonuniform bursts of equal duration and number of pulses with nonuniformly spaced inner pulses ("nonfrequency-specific patterns," interpulse intervals between pulses 24, 52, and 24 ms, respectively). Importantly, the first and last pulses of both types of bursts were always delivered 118 and 16 ms before target onset, respectively. A frameless stereotaxic neuronavigation system (eximia, Nextim, Helsinki, Finland) was used to guide and maintain on each individual and across experimental blocks the coil location on a set of specific FEF coordinates (Talairach $x = 31$, $y = -2$, $z = 47$) (Fig. 1b). For all patterns and blocks, TMS intensity was initially set up at 45% of the TMS maximal machine output. Occasionally in some participants, intensity had to be slightly decreased to abolish temporal involuntary muscle activation, involuntary blinks, or others types of facial sensations. Participants were stimulated at an average intensity of $44 \pm 1.5\%$ (which corresponded to $72 \pm 13\%$ of their resting motor threshold). In half of the trials, a short burst of 4 real TMS pulses was applied directly to the right FEF (active TMS trials). In the other half (sham TMS trials), the same burst was delivered by a second TMS coil placed next to the stimulation site, with the coil surface perpendicular to the head surface, preventing the magnetic field from reaching the skull and stimulating the brain. The order of active and sham TMS trials was randomized (Chanes et al. 2013).

After the delivery of the TMS burst and the presentation of the Gabor, participants were first required to determine with their right hand the "right" or "left" orientation of the "Gabor" lines ("discrimination task") as accurately as possible. They were also forced to guess a response, even when the target was not present or they did not consciously perceive it. Then, participants were requested to report with their left hand whether they perceived the Gabor on the "left," or the "right" of the fixation cross, or they did not see it ("detection task") (Fig. 1a). Discrimination performance was analyzed through accuracy measures (correct grating orientation categorization). Perceptual sensitivity (d') and response bias (beta) used in signal detection theory served to assess the modulation of conscious visual detection. Participants were requested to keep their gaze on the fixation cross throughout the trial. Eye movements were controlled by an eye-tracker system, and fixation was considered broken when gaze position was recorded outside the central box, that is, 3° of angle away from the fixation cross horizontally, and 2.75° vertically (Chanes et al. 2013). Each of the 2 blocks consisted of 200 trials, and included 40 trials in which the target was absent (20% of the trials of each block). Participants were allowed to take a short break every 40 trials and at the end of each sub-block they received feedback about their performance and fixation violation rates.

MRI Acquisition

Diffusion MRI scans were obtained on a 3-T MRI scanner (Tim Trio, Siemens Healthcare, Erlangen, Germany) located at the CENIR (Centre de Neuro-Imagerie de Recherche) at the Hôpital de la Pitié Salpêtriére, in Paris (France). Using a 32-channel array coil and a maximum gradient of 28 mT/m, diffusion weighting was isotropically distributed along 60 directions and 6 nondiffusion-weighted volumes were acquired. The first $b0$ image served as an anatomical reference for the correction of eddy currents. Imaging parameters were as follows: voxel size = $1.7 \times 1.7 \times 1.7$, repetition time (TR) = 12 800 ms, echo time (TE) = 88 ms, $b = 1500$ s/mm^2, and matrix size = $129 \times 129 \times 71$. Each set of images contained 71 contiguous slices with a 1.7-mm thickness. Total acquisition time was 14 min and 43 s. A three-dimensional (3D) structural T_1-weighted MRI also employed to neuronavigate the TMS coil was acquired on each subject (TR = 2300 ms, TE = 4.18 ms, field of view = 265 mm, matrix size = 256×256 and 176 sagittal slices with 1 mm thickness).

Data Processing and Estimation of Fiber Orientation

Diffusion images were corrected for head motion and eddy current distortions using affine registration to the first nondiffusion-weighted volume implemented in the FSL software package (FSL 4.1.6—www.fmrib.ox.ac.uk/fsl/). Spatial deformations of the DTI dataset due to susceptibility artifacts were corrected with nonlinear deformation computed from the diffusion images to match the T_1-weighted volume using the Freesurfer Software (Freesurfer 5.0.0, http://surfer.nmr.mgh.harvard.edu/). A spherical deconvolution approach (Tournier et al. 2007) with a modified damped version of the Richardson-Lucy algorithm (Dell'acqua et al. 2010) was employed to estimate fiber orientation in each white matter voxel. This approach was chosen to allow the reconstruction of several orientations in voxels containing different populations of crossing fibers. An absolute and a relative threshold were used to exclude spurious local maxima of fiber orientation distribution (Thiebaut de Schotten et al. 2011).

Tractography

Whole-brain tractography was performed starting from every voxel with at least one fiber orientation as a seed voxel. From these voxels and for each fiber orientation, a modified fiber assignment using a continuous tracking algorithm was used to reconstruct streamlines by sequentially piecing together discrete and shortly spaced estimates of fiber orientation forming continuous trajectories. When entering a region with crossing white matter bundles, the algorithm followed the orientation vector of least curvature. Streamlines were halted when a voxel without fiber orientation was reached or when the curvature between 2 steps exceeded a threshold of 45°. The software estimating and reconstructing the orientation vectors and the trajectories from diffusion MRI was implemented in Matlab 7.8 (MathWorks, Natick, MA, USA). Each SLF branch was normalized to the Montreal Neurological Institute (MNI) mean brain volume using SPM (http://www.fil.ion.ucl.ac.uk/spm) to create a mean tractography image.

SLF Dissection

A previously validated method (Thiebaut de Schotten et al. 2011) was used to dissect the 3 branches of the SLF. Fasciculi from both hemispheres were considered, as visual detection enhancements induced by rhythmic TMS patterns proved bilateral (Chanes et al. 2013). To delineate the SLF I, II, and III, 3 regions of interest (ROIs) encompassing the white matter of the superior, middle, and inferior/precentral frontal gyri were outlined on a coronal section at the anterior commissure's level. A parietal ROI was also delineated on a coronal section at the level of the posterior commissure. This "AND" ROI was common to the 3 branches of the SLF. A temporal ROI was used to exclude streamlines of the arcuate fasciculus, which are not integrated in fronto-parietal white matter projections. When required, an ROI encompassing the internal and external capsules was employed to eliminate descending fibers.

White Matter Pathways—Behavioral Correlations

The volume of the 3 branches of the SLF was determined and divided by the total tracked white matter volume of each participant. The relative conscious visual detection sensitivity gains ($\Delta d'$) induced by active versus sham neurostimulation was used to estimate perceptual improvements of conscious vision caused by high-beta (30 Hz) frontal TMS patterns, which demonstrated significant visual sensitivity (d') increases at the group level. Similar correlations were also performed for the modulation of identical visual outcome measures by nonfrequency-specific frontal control bursts, which did not reach statistical significance at the group level. A Shapiro–Wilk test was used to verify the Gaussian distribution of these variables (all $P > 0.12$). The Pearson's correlation coefficient between tract volume and $\Delta d'$ was calculated for each branch of the SLF white matter tract (JMP 10.0.0, SAS, Cary, NC, USA). Bonferroni post hoc correction was used to compensate for the family-wise error rate in multiple comparisons (uncorrected *$P < 0.05$; corrected **$P < 0.05/12 \approx 0.004$). To provide additional and convincing proof of the robustness of our statistically significant correlation, a permutation test (Groppe et al. 2011) based on Pearson's correlation coefficient with 5000 permutations was also applied. We permuted the SLF I pathway volume in both hemispheres within our group of 12 participants and recalculated the correlation with each new version of this

modified dataset. The null hypothesis of the permutation test is that the correlation obtained with the initial order is as likely as the correlation obtained with random permutations. The skipped correlation procedure (Rousselet and Pernet 2012), which performs a robust Pearson correlation on data cleaned up for bivariate outliers, was also employed. The correlation coefficients between specific tract volume and visual modulations induced by either frequency-specific or nonfrequency-specific patterns were statistically compared using the method reported in Steiger et al. (1980). Finally, a General Linear Model (GLM) implemented on Matlab 7.11.0 (MathWorks) was also used to further verify the correlation of a given pathway with conscious visual outcome measures, independently of the participant's age, motor threshold, other SLF branch volumes, and the total brain's tracked white matter volume.

Results

We first analyzed the normalized volume of each of the 3 SLF branches across our group of participants. When comparing the 2 hemispheres, a previously reported branch-specific right hemispheric lateralization pattern (Thiebaut de Schotten et al. 2011) involving the SLF III ($t = 3.93$; $P = 0.002$, df = 11) but neither the SLF I nor the SLF II branches ($t < 1$) was found. This finding, which replicates such influential outcome, suggests the reproducibility of the white matter tracking method employed in this study for the SLF. We then calculated performance differences between active and sham rhythmic 30-Hz TMS patterns to obtain the relative visual sensitivity gain ($\Delta d'$) for conscious detection. Interestingly, this measure significantly correlated with the right hemisphere's SLF I volume ($r = -0.83$; $P < 0.001$, Bonferroni corrected), whereas visual performance correlations with the SLF II ($r = 0.17$; $P = 0.60$) and the SLF III ($r = -0.49$; $P = 0.10$) tract volume failed to reach statistical significance. A significant correlation between $\Delta d'$ and the left hemisphere's SLF I ($r = -0.68$; $P = 0.015$, uncorrected), but neither with the SLF II ($r = -0.33$; $P = 0.29$) nor the SLF III ($r = 0.03$; $P = 0.92$) was also found. Importantly, similar significance for the right ($r = -0.83$; $t = -4.78$) and left SLF I branch ($r = -0.68$; $t = -2.91$) was also found when the skipped correlation approach was employed on this same dataset.

Correlations between individual visual sensitivity (d') modulations induced by nonfrequency-specific TMS patterns and white matter pathway volumes were also tested. Importantly, none of the 6 white matter pathways' volume significantly correlated with the above-mentioned perceptual outcome measure (right SLF I: $r = -0.39$; $P = 0.21$, left SLF I: $r = -0.24$; $P = 0.44$, right SLF II: $r = 0.50$; $P = 0.09$, left SLF II: $r = -0.19$; $P = 0.55$, right SLF III: $r = -0.40$; $P = 0.19$, and left SLF III: $r = -0.10$; $P = 0.74$).

To further corroborate that this effect was specifically related to stimulation frequency, we confirmed that the correlation coefficient between the right SLF I volume and visual modulations induced by frequency-specific TMS pattern was significantly higher than the one established between this same branch volume and visual performance shifts yielded by nonfrequency-specific neurostimulation patterns ($P = 0.03$). Moreover, a permutation test confirmed these results for the correlations between the right ($P = 0.0032$) and left SLF I ($P = 0.024$) and the impact of spatio-temporal right frontal beta activity on visual sensitivity shifts. Finally, a multiple linear regression analysis based on the GLM t-test with the 2 statistically significant pathways, the right and left SLF I, as explanatory variables and the nonsignificant pathways, participant's age, motor threshold, and total tracked brain volume as confound regressors confirmed once more that only the dorsal-

most SLF branch (SLF I) covaried significantly with conscious visual performance outcomes ($t = -3.32$; $P = 0.005$; df = 8, Bonferroni corrected) (Fig. 2).

To avoid any ceiling effects, target contrast was adjusted prior to task onset and during the task itself, every 20 trials, to keep steady performance rates at 50% of correct conscious detection (see Chanes et al. 2013 for details). Importantly, individual contrast levels required to ensure such specific levels of performance did neither correlate with white matter pathway volumes for the 6 branches analyzed in the study ($r = -0.49$, $P = 0.10$), nor with the effects of frequency-specific frontal TMS patterns on visual sensitivity ($r = 0.45$, $P = 0.14$).

As indicated elsewhere (Quentin et al. 2013), others sources of interindividual variability (e.g. the intrinsic excitability levels of the stimulated frontal region and its associated networks, cortical shape, the distribution of cerebro-spinal fluid, or the relative orientation of neuronal layers with regard to the coil surface, to provide some examples) cannot be accurately characterized with current human neuroimaging methods and may have contributed to some extent to variability in TMS efficacy and by extension to performance variability (Bijsterbosch et al. 2012).

Discussion

Our data indicate that the ability of spatio-temporal right frontal neurostimulation patterns to induce sensitivity improvements of conscious vision is primarily modulated by the volume of the SLF I white matter branch, connecting the FEF and the IPS regions. This result applies only to the impact of frequency-specific frontal beta patterns at 30 Hz, as no significant correlations were found for the effects of nonfrequency-specific patterns delivered to this same frontal location.

Like only the correlation with the right SLF I survived a Bonferroni correction and oscillation patterns were induced on the right FEF, further analyses focused on the right hemisphere's SLF I tract. It would be tempting to interpret the uncorrected correlation with the left SLF I tract as the substrate of the bilateral visual detection improvements reported by Chanes et al. (2013). Nonetheless, since the first branch of the SLF has been shown not to be anatomically lateralized either to the left or the right hemisphere (Thiebaut de Schotten et al. 2011), this trend could be simply due to the fact that the volumes of these 2 tracts are strongly correlated ($P = 0.001$).

Like in a recent study employing single-pulse TMS (Quentin et al. 2013), the correlation between the behavioral impact of rhythmic TMS on d' and the SLF I volume proved to be negative. Despite differences in the stimulation patterns employed on each case, the current outcome provides additional experimental support in favor of an inverse association between TMS modulated behaviors and white matter connectivity (Quentin et al. 2013). This result might seem counterintuitive, as larger tract volumes or higher probability of connection acting under physiological conditions have been often associated with more effective connectivity and information transfer (Glasser and Rilling 2008; Thiebaut de Schotten et al. 2011). Alternatively, however, thinner pathways could prove more efficient in conveying neural signal particularly when those are artificially induced by nonsufficiently focal noninvasive neurostimulation sources. Indeed, as hypothesized elsewhere (Wagner et al. 2009), smaller and less populous white matter tracts, with features and properties which may be innately determined (van Kooij et al. 2011) and also shaped by postnatal training
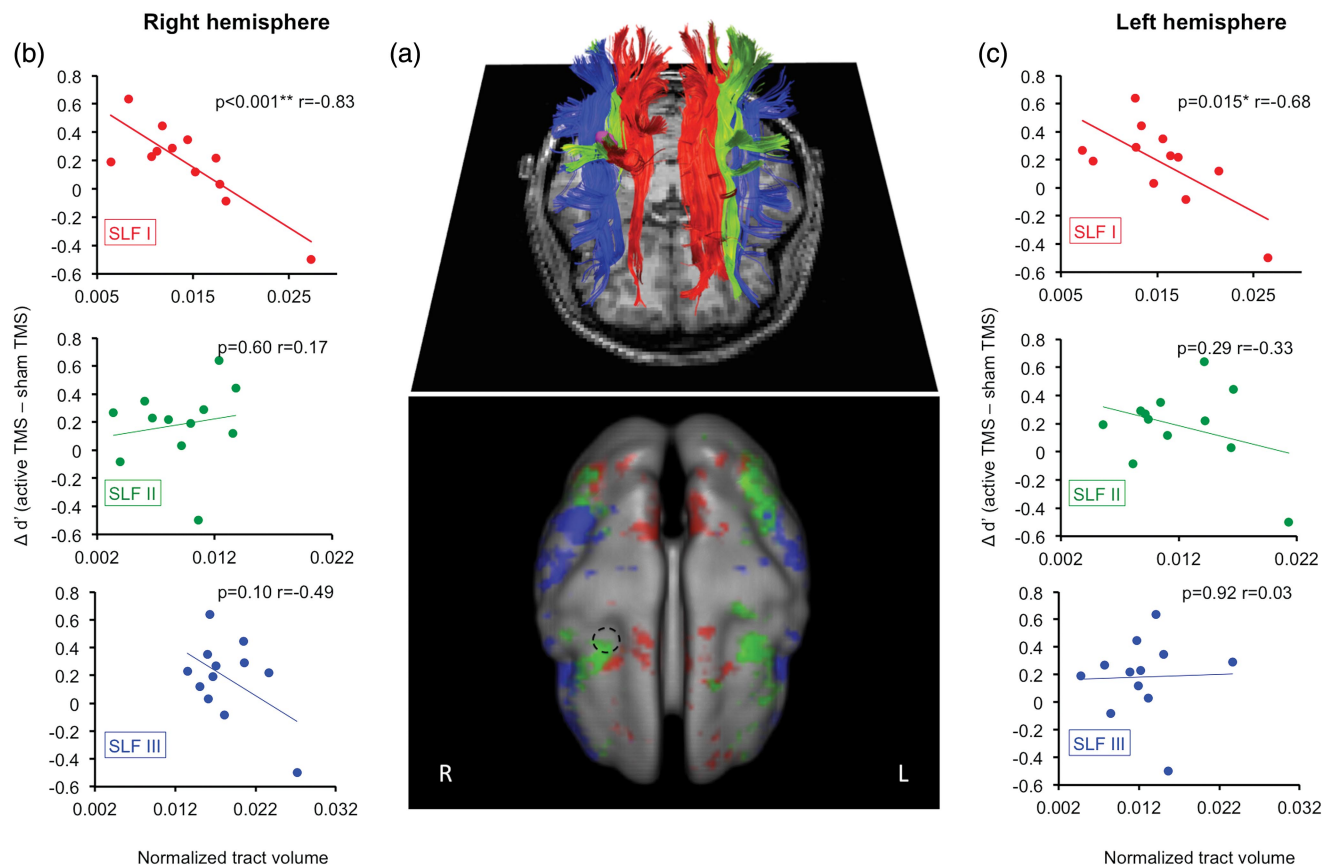
Figure 2. Correlations between white matter diffusion imaging data and conscious visual detection performance associated with the manipulation of frontal oscillatory activity. (*a*) Upper middle panel: Tractographic rendering of the 3 branches of the SLF (SLF I in red, SLF II in green, and the SLF III in blue) in a representative participant. The purple region signals the cortical location of the stimulated area; lower middle panel: top view, image representing on a 3D MNI white matter template the mean cortical projections of the 3 SLF branches (SLF I in red, SLF II in green, and the SLF III in blue). The black circle signals the cortical location of the stimulated region, the right FEF. (Right and left panels, *b* and *c*) Correlation plots between conscious visual detection sensitivity gains ($\Delta d'$) (d' for active TMS $- d'$ for sham TMS) and the normalized volume of each of the 3 SLF branches. Correlations are presented for the right (*b*) and the left (*c*) hemispheres, respectively. Note that only the right SLF I ($r = -0.83$; $P < 0.001$, Bonferroni corrected) and left SLF I ($r = -0.68$; $P = 0.015$, uncorrected) branches linking the FEF to the IPS regions showed a significant correlation between white matter volume and visual sensitivity gains. Asterisk indicates: * uncorrected ($P < 0.05$); ** Bonferroni corrected ($P < 0.05/12$).

experience (Imfeld et al. 2009), could prove less prone to "parasitic" phenomena such as interferences caused by center-surround inhibitory effects of fibers running within the same tract, when forcedly activated by TMS. Such projections could convey less noisy and more robust signals to postsynaptic parietal and occipital sites (see Quentin et al. 2013 for further discussion of this issue). If the latter remains a plausible hypothesis, one needs to remain very cautious when attempting to derive physiological explanations from purely structural data (Jbabdi and Johansen-Berg 2011; Jones et al. 2012) and further experiments are absolutely required to better understand the basis of this association. Alternatively, this result could also be explained by the fact that participants with larger white matter tracts may benefit from a more selective top-down control on visual performance, allowing higher baseline levels of detection performance which would limit the leverage to experience further visual sensitivity increases. This explanation seems, however, implausible as no significant correlations were found, neither between the stimulus contrast levels required to keep baseline visual detection rates constant and white matter pathway volumes, nor between those contrast levels and the visual impact of frequency-specific frontal beta patterns.

Most importantly, our results are novel and could prove relevant to establish potential links between cerebral

synchronization and the anatomical pathways conveying such activity throughout fronto-parietal networks of the right hemisphere. Focal noninvasive neurostimulation by TMS has already demonstrated a primary impact on the stimulated region that spreads remotely, and its ability to modulate an entire network of areas connected by anatomical white matter projections in animals (Valero-Cabré et al. 2005, 2007) and humans (Quentin et al. 2013). Moreover, recent monkey electrophysiological evidence and causal neurostimulation studies in humans support frequency-specific oscillatory activity in top-down spatial orienting and visual performance (Buschman and Miller 2007; Romei et al. 2012; Chanes et al. 2013). Based on our own observations, and prior electrophysiological monkey and human evidence (Buschman and Miller 2007; Phillips and Takeda 2009), we here present the working hypothesis that high-beta oscillation patterns entrained in a right frontal region might not remain local, but likely spread out along the dorsal attentional network, and that such activity patterns could be subtended by fibers of the first branch of the SLF.

In the past, similar modulations of visual performance have also been explained by long-range connectivity effects of stimulated frontal and parietal regions operating on the input gain and signal strength of visual stimuli processed at occipital and tectal

regions ([Ruff et al. 2006](#); [Quentin et al. 2013](#)). The current results call, however, for a hypothesis able to better substantiate in physiological terms the relation between white matter connectivity and interregional synchrony between frontal and the dorsal and posterior portions of the parietal cortex. Prior reports have suggested that visual cognition relies on fronto-parietal synchronization, and that such processes increase the coupling between brain regions, enhancing sensory evidence ([Fries 2005](#); [Buschman and Miller 2007](#); [Miller and Buschman 2013](#)). Consequently, anatomical differences in white matter tracts may impact how spatio-temporal patterns are reverberated across extended brain networks and could determine their ability to modulate conscious visual behaviors. Interestingly, tract volume is associated with factors such as axonal diameter and myelination rates, which determine the conduction speed of neural signals across white matter pathways. In this particular framework, our data may suggest that interregional synchronization processes entrained at a specific frequency are strongly influenced by the biophysical properties of the specific white matter tracts established between sets of cortical regions and their derived impact on time lag and conduction velocity, indicating that greater axonal conduction velocity may allow for more reliable synchronization at higher oscillation frequencies ([Zaehle and Herrmann 2011](#)). In our study, this notion would entail, if proven correct, that the visual consequences of rhythmic high-beta frontal activity patterns specifically delivered at 30 Hz depend on the individual conduction time lag between frontal and parietal regions and the ulterior ability of this network to synchronize activity at this specific frequency band. Consequently, individual performance under rhythmic TMS patterns could depend on the suitability of the entrained oscillation frequency to the structural and physiological properties of white matter tracts mediating interregional coupling and synchrony. Individual differences in anatomical connectivity and interregional conduction time lag could also explain the relatively broad bandwidth of oscillation frequencies, which in electrophysiological studies have been associated (within a given band such as alpha, beta, or gamma) with processes such as visuo-spatial attention, perception, and visual consciousness ([Wyart and Tallon-Baudry 2009](#); [Thut et al. 2011](#)). Although this was out of the scope of the current study, by ascertaining an exquisite dependency between behavioral outcomes and rhythmic neurostimulation bursts at several values slightly below and above a central 30-Hz pattern, co-varying with individual SLF I measures could provide further causal confirmation in favor of this interesting hypothesis.

Nonetheless, in the absence of interleaved TMS-electrophysiological online evidence, a mechanistic hypothesis based on synchronization within the fronto-parietal network cannot be here fully demonstrated. Thus, as previously hypothesized in this discussion, effects on perception could also reflect a local FEF impact and a top-down propagation from this site that is dependent of fronto-parietal fibers and stronger under the influence of beta-stimulation patterns, without any necessary contribution of coherent beta activity from parietal sites.

In summary, our study suggests a strong association between fronto-parietal white matter anatomy, rhythmic brain activity, and the emergence of conscious visual perception, and supports a future role for individual white matter patterns in tailoring the frequency of rhythmic neurostimulation in future research and clinical applications.

References

Bijsterbosch JD, Barker AT, Lee K-H, Woodruff PWR. 2012. Where does transcranial magnetic stimulation (TMS) stimulate? Modelling of induced field maps for some common cortical and cerebellar targets. Med Biol Eng Comput. 50:671–681.

Buschman TJ, Miller EK. 2007. Top-down versus bottom-up control of attention in the prefrontal and posterior parietal cortices. Science. 315:1860–1862.

Chanes L, Chica AB, Quentin R, Valero-Cabré A. 2012. Manipulation of pre-target activity on the right frontal eye field enhances conscious visual perception in humans. PLoS ONE. 7:e36232.

Chanes L, Quentin R, Tallon-Baudry C, Valero-Cabré A. 2013. Causal frequency-specific contributions of frontal spatiotemporal patterns induced by non-invasive neurostimulation to human visual performance. J Neurosci. 33:5000–5005.

Chica AB, Bartolomeo P, Valero-Cabré A. 2011. Dorsal and ventral parietal contributions to spatial orienting in the human brain. J Neurosci. 31:8143–8149.

Corbetta M, Patel G, Shulman GL. 2008. The reorienting system of the human brain: from environment to theory of mind. Neuron. 58:306–324.

Dell'acqua F, Scifo P, Rizzo G, Catani M, Simmons A, Scotti G, Fazio F. 2010. A modified damped Richardson-Lucy algorithm to reduce isotropic background effects in spherical deconvolution. Neuroimage. 49:1446–1458.

Fries P. 2005. A mechanism for cognitive dynamics: neuronal communication through neuronal coherence. Trends Cogn Sci (Regul Ed). 9:474–480.

Glasser MF, Rilling JK. 2008. DTI tractography of the human brain's language pathways. Cereb Cortex. 18:2471–2482.

Groppe DM, Urbach TP, Kutas M. 2011. Mass univariate analysis of event-related brain potentials/fields I: a critical tutorial review. Psychophysiology. 48:1711–1725.

Imfeld A, Oechslin MS, Meyer M, Loenneker T, Jancke L. 2009. White matter plasticity in the corticospinal tract of musicians: a diffusion tensor imaging study. Neuroimage. 46:600–607.

Jbabdi S, Johansen-Berg H. 2011. Tractography—where do we go from here? Brain Connect. 1:169–183.

Jones DK, Knösche TR, Turner R. 2012. White matter integrity, fiber count, and other fallacies: The do's and don'ts of diffusion MRI. Neuroimage. 73:239–254.

Kincade JM, Abrams RA, Astafiev SV, Shulman GL, Corbetta M. 2005. An event-related functional magnetic resonance imaging study of voluntary and stimulus-driven orienting of attention. J Neurosci. 25:4593–4604.

Makris N, Kennedy DN, McInerney S, Sorensen AG, Wang R, Caviness VS, Pandya DN. 2005. Segmentation of subcomponents within the superior longitudinal fascicle in humans: a quantitative, in vivo, DT-MRI study. Cereb Cortex. 15:854–869.

Miller EK, Buschman TJ. 2013. Cortical circuits for the control of attention. Curr Opin Neurobiol. 23:216–222.

Phillips S, Takeda Y. 2009. Greater frontal-parietal synchrony at low gamma-band frequencies for inefficient than efficient visual search in human EEG. Int J Psychophysiol. 73:350–354.

Quentin R, Chanes L, Migliaccio R, Valabregue R, Valero-Cabre A. 2013. Fronto-tectal white matter connectivity mediates facilitatory effects of non-invasive neurostimulation on visual detection. NeuroImage. 82:344–354.

Romei V, Gross J, Thut G. 2010. On the role of prestimulus alpha rhythms over occipito-parietal areas in visual input regulation: correlation or causation? J Neurosci. 30:8692–8697.

Romei V, Thut G, Mok RM, Schyns PG, Driver J. 2012. Causal implication by rhythmic transcranial magnetic stimulation of alpha frequency in feature-based local vs. global attention. Eur J Neurosci. 35:968–974.

Rousselet GA, Pernet CR. 2012. Improving standards in brain-behavior correlation analyses. Front Hum Neurosci. 6:119.

Ruff CC, Blankenburg F, Bjoertomt O, Bestmann S, Freeman E, Haynes J-D, Rees G, Josephs O, Deichmann R, Driver J. 2006. Concurrent TMS-fMRI and psychophysics reveal frontal influences on human retinotopic visual cortex. Curr Biol. 16:1479–1488.

Scholz J, Klein MC, Behrens TEJ, Johansen-Berg H. 2009. Training induces changes in white matter architecture. Nat Neurosci. 12:1370–1371.

Steiger JH. 1980. Tests for comparing elements of a correlation matrix. Psychol Bull. 87:245–251.

Thiebaut de Schotten M, Dell'Acqua F, Forkel S, Simmons A, Vergani F, Murphy DG, Murphy D, Catani M. 2011. A lateralized brain network for visuo-spatial attention. Nat Neurosci. 14:1245–1246.

Thiebaut de Schotten M, Dell'Acqua F, Valabregue R, Catani M. 2012. Monkey to human comparative anatomy of the frontal lobe association tracts. Cortex. 48:82–96.

Thut G, Veniero D, Romei V, Miniussi C, Schyns P, Gross J. 2011. Rhythmic TMS causes local entrainment of natural oscillatory signatures. Curr Biol. 21:1176–1185.

Tournier J-D, Calamante F, Connelly A. 2007. Robust determination of the fibre orientation distribution in diffusion MRI: non-negativity constrained super-resolved spherical deconvolution. Neuroimage. 35:1459–1472.

Tuch DS, Salat DH, Wisco JJ, Zaleta AK, Hevelone ND, Rosas HD. 2005. Choice reaction time performance correlates with diffusion anisotropy in white matter pathways supporting visuospatial attention. Proc Natl Acad Sci USA. 102:12212–12217.

Valero-Cabré A, Payne BR, Pascual-Leone A. 2007. Opposite impact on 14C-2-deoxyglucose brain metabolism following patterns of high and low frequency repetitive transcranial magnetic stimulation in the posterior parietal cortex. Exp Brain Res. 176:603–615.

Valero-Cabré A, Payne BR, Rushmore J, Lomber SG, Pascual-Leone A. 2005. Impact of repetitive transcranial magnetic stimulation of the parietal cortex on metabolic brain activity: a 14C-2-DG tracing study in the cat. Exp Brain Res. 163:1–12.

Van Kooij BJM, van Pul C, Benders MJNL, van Haastert IC, de Vries LS, Groenendaal F. 2011. Fiber tracking at term displays gender differences regarding cognitive and motor outcome at 2 years of age in preterm infants. Pediatr Res. 70:626–632.

Wagner T, Rushmore J, Eden U, Valero-Cabre A. 2009. Biophysical foundations underlying TMS: setting the stage for an effective use of neurostimulation in the cognitive neurosciences. Cortex. 45: 1025–1034.

Wyart V, Tallon-Baudry C. 2009. How ongoing fluctuations in human visual cortex predict perceptual awareness: baseline shift versus decision bias. J Neurosci. 29:8715–8725.

Zaehle T, Herrmann CS. 2011. Neural synchrony and white matter variations in the human brain—relation between evoked gamma frequency and corpus callosum morphology. Int J Psychophysiol. 79:49–54.